Carbohydrate Polymers 87 (2012) 328–335

Contents lists available at ScienceDirect

Carbohydrate Polymers

journal homepage: www.elsevier.com/locate/carbpol

Impact of magnetic nanofillers in the swelling and release properties of κ-carrageenan hydrogel nanocomposites

Ana L. Daniel-da-Silva*, Joana Moreira, Rodrigo Neto, Ana C. Estrada, Ana M. Gil, Tito Trindade

Department of Chemistry, CICECO, University of Aveiro, 3810-193 Aveiro, Portugal

ARTICLE INFO

Article history:
Received 3 May 2011
Received in revised form 11 July 2011
Accepted 26 July 2011
Available online 3 August 2011

Keywords:
Carrageenan
Hydrogels
Nanocomposites
Swelling
Drug release
Magnetite

ABSTRACT

Natural polysaccharides such as κ-carrageenan are an important class of biomaterials for drug delivery. The incorporation of magnetic nanoparticles in polysaccharide hydrogels is currently being explored as a strategy to confer to the hydrogels novel functionalities valuable for specific bio-applications. Within this context, κ-carrageenan magnetic hydrogel nanocomposites have been prepared and the effect of magnetic (Fe_3O_4) nanofillers in the swelling of the hydrogels and in the release kinetics and mechanism of a model drug (methylene blue) has been investigated. *In vitro* release studies demonstrated the applicability of the composites in sustained drug release. The mechanism controlling the release seems to be determined by the strength of the gel network and the extent of gel swelling, both being affected by the incorporation of nanofillers. Furthermore, it was demonstrated that the release rate and profile could be tailored using variable Fe_3O_4 nanoparticles load. Thus, this seems to be a promising strategy for the development of drug delivery systems with tailored released behavior.

1. Introduction

Hydrogels are three-dimensional networks of water-soluble polymers exhibiting unique physicochemical properties that make them advantageous in certain biomedical applications, including drug delivery (Hamidi, Azadi & Rafiei, 2008; Hoare & Kohane, 2008). In this context, hydrogels valuable properties include hydrophilicity, high water absorbing capacity, soft consistency, biocompatibility and biodegradability. Since gel fabrication usually requires mild conditions some biopolymers are suitable to encapsulate biomolecules. In order to tailor the rate of gel swelling or degradation and to control the release of encapsulated molecules, the hydrogel network can be chemically modified using a number of strategies that include their use in nanocomposites.

The addition of magnetic nanoparticles (NPs) such as magnetite (Fe_3O_4) is of extremely importance for biomedical applications and results in hydrogel nanocomposites that will be responsive to external magnetic stimuli. An immediate benefit arising from the incorporation of magnetic NPs into hydrogels is the magnetically driven drug transport which enables site specific drug delivery to be envisaged (Polyak & Friedman, 2009). Furthermore, adequate magnetic stimuli can be used to induce controllable deformations of the hydrogel matrix and remotely control the release of encapsulated therapeutic agents (Liu, Hu, Liu, Liu, & Chen, 2006; Zrínyi, 2000). Due to the above-mentioned reasons hydrogel nanocomposites are attractive in relation to the development of site-specific and/or time-controlled delivery systems (Frimpong & Hilt, 2007; Satarkar, Biswal, & Hilt, 2010). In addition, magnetite nanoparticles will confer new functionalities to the resulting nanocomposites which are valuable for other applications including medical imaging (Saboktakin, Tabatabaie, Maharramov, & Ramazanov, 2010; Shen et al., 2005).

The therapeutic success of a drug delivery system is determined by its drug release kinetics which depends on the release mechanism. Parameters affecting the diffusivity of the drug and the physical properties of the hydrogel (e.g. molecular weight of drug and polymer, polymer concentration, crosslink density of polymer, interactions drug–polymer) determine the dominant mechanism (Lin & Metters, 2006). The majority of the above mentioned factors have been studied for several hydrogels (Hoare & Kohane, 2008; Lin & Metters, 2006; Peppas, Bures, Leobandung, & Ichikawa, 2000). However, although hydrogel nanocomposites containing magnetic NPs have been increasingly investigated for drug delivery applications (Bertoglio, Jacobo, & Daraio, 2010; Hu, Liu, Liu, & Chen, 2007; Saboktakin et al., 2010), the role of these nanofillers on the release mechanism from hydrogels is not clear.

Carrageenan comprises a family of linear water-soluble sulfated polysaccharides extracted from red seaweeds that have the ability to form thermoreversible hydrogels and are extensively used as gelling agent in food and pharmaceutical industries (Piculell, 1995).

* Corresponding author. Tel.: +351 234 370 368; fax: +351 234 370 084.
E-mail address: ana.luisa@ua.pt (A.L. Daniel-da-Silva).

0144-8617/$ – see front matter © 2011 Elsevier Ltd. All rights reserved.
doi:10.1016/j.carbpol.2011.07.051

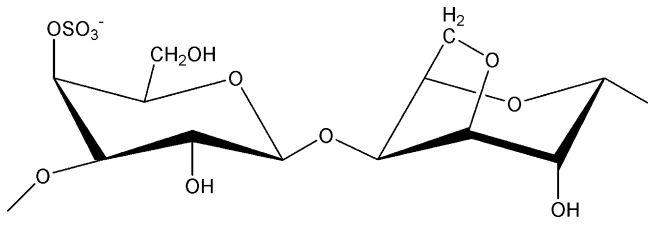

Fig. 1. The structural disaccharide unit of κ-carrageenan.

Within the carrageenan family, κ-carrageenan (Fig. 1) originates the strongest gels and, hence, in the last decade this biopolymer has been investigated as a carrier for controlled drug release, either on its own (Daniel-da-Silva, Ferreira, Gil, & Trindade, 2011; Gupta, Hariharan, Wheatley, & Price, 2001; Leong et al., 2011; Keppeler, Ellis, & Jacquier, 2009; Sankalia, Mashru, Sankalia, & Sutariya, 2006; Santo et al., 2009), or mixed with other carrageenans (Nannaki, Karava, Kalantzi, & Bikiaris, 2010) or polymers (Liu, Zhu, Wei, & Lu, 2009; Mohamadnia, Zohuriaan-Mehr, Kabiri, Jamshidi, & Mobedi, 2007; Rasool, Yasin, Heng, & Akhter, 2010; Tapia, Corbalan, Costa, Gai, & Yazdani-Pedram, 2005). Our recent studies on κ-carrageenan/magnetite nanocomposites have revealed that the resulting nanocomposites form thermoreversible hydrogels with potential for applications in magnetically and/or thermally activated drug release (Daniel-da-Silva et al., 2008, 2009). In the present work we report the study of the swelling properties and kinetics of the release of a model drug from magnetite hydrogel nanocomposites, using κ-carrageenan as the matrix and methylene blue as model drug. The main aim of this work was to investigate the effect of Fe_3O_4 NPs on the swelling and kinetics and release mechanism of a model drug from κ-carrageenan based nanocomposite hydrogels. Fe_3O_4 NPs have been selected as nanofillers due to their relevance in the development of new composite materials for bio-applications.

2. Materials and methods

2.1. Materials

κ-Carrageenan (300,000 g/mol Fluka Chemie), methylene blue ($C_{16}H_{18}ClN_3S{\cdot}3H_2O$) (Riedel-de-Haën), ferric chloride hexahydrated ($FeCl_3{\cdot}6H_2O$) (>99%, Sigma–Aldrich), ferrous chloride tetrahydrated ($FeCl_2{\cdot}4H_2O$) (>99%, Sigma–Aldrich), potassium hydroxide (KOH) (>86%, Pronalab), potassium chloride (KCl) (>99%, Sigma–Aldrich), phosphate buffered saline (PBS) (pH 7.4, Sigma–Aldrich) and sodium azide (NaN_3) (99%, Sigma–Aldrich) were used as received without any further purification.

2.2. Synthesis of magnetic nanoparticles

The magnetic iron oxide NPs were produced by chemical co-precipitation. In a typical procedure 0.5 g of iron(II) chloride tetrahydrated were added to 40.0 mL of acidified iron(III) chloride (0.1 M), freshly prepared in deoxygenated water at 70 °C, under a nitrogen atmosphere. Ferrous ion was added in slight excess of the magnetite stoichiometric molar ratio ($Fe^{3+}/Fe^{2+} = 2{:}1$) in order to account for spontaneous oxidation of Fe^{2+}. Then 20 mL of 1 mol dm^{-3} potassium hydroxide was added immediately, to adjust the pH to 10. The reaction was allowed to proceed over 30 min, at 70 °C, under permanent stirring and nitrogen atmosphere. The mixture turned black which, together with the observed magnetic properties under the influence of a magnet, indicated the presence of magnetite (Fe_3O_4), as reported elsewhere (Daniel-da-Silva et al., 2008). After synthesis the particles were consecutively washed with distilled water and separated magnetically, in order to eliminate adsorbed salts and unreacted iron species.

Table 1
Carrageenan hydrogels and corresponding synthesis conditions.

Sample designation	$C_{carrageenan}$ (g/L)	C_{KCl} (M)	Nanofiller	% (w/w) ($m_{NPs}/m_{polymer}$)
K20	20	1	–	0
K40	40	1	–	0
K40_2	40	2	–	0
K40_MGN	40	1	Fe_3O_4	0.025
K40_MGN100	40	1		2.50

2.3. Preparation of κ-carrageenan nanocomposites

The nanocomposites were prepared by blending the Fe_3O_4 NPs with the polymer matrix as follows. A methylene blue (MB) 0.33 mg/mL solution containing the NPs in the required concentration was firstly prepared. Then 2.5 mL of this suspension was added to 25 mL of a 40 g/L κ-carrageenan solution under sonication in an ultrasonic processor Cole Parmer (USA), at 80 °C, followed by the addition of 2.5 mL of KCl 1 M to promote the gelation of κ-carrageenan and stirring. Afterwards 2.5 mL of the composite was transferred to a cylindrical glass vial (Ø 17 mm) and allowed to cool down to room temperature to induce gelation of the composite. The gel samples were frozen at −5 °C for 24 h and lyophilized. The final freeze dried discs had approximately 15 mm diameter and 8 mm width.

The synthesis conditions for the carrageenan carriers here prepared are listed in Table 1. The load of Fe_3O_4 nanoparticles was varied. For sake of comparison, carriers comprising only κ-carrageenan, K^+ ions and MB were also prepared following the procedure described above with no incorporation of the dispersed phase (blank hydrogel). The concentration of κ-carrageenan and K^+ ions was varied in order to evaluate the influence of the matrix composition.

2.4. Swelling studies

The swelling measurements were carried out by immersion of lyophilized hydrogel discs in PBS 0.01 M pH 7.4 and PBS rich in K^+ ions (1 M) at 37 °C. At the required intervals of time, the samples were removed from the solution and wiped with filter paper to remove the excess of water before being weighted. The swelling ratio (Q) was calculated from Eq. (1)

$$Q = \frac{W_s - W_d}{W_d} \quad (1)$$

where W_d and W_s is the weight of the lyophilized and swollen gel, respectively. The equilibrium swelling ratio (Q_{equil}) was determined at the point the hydrated gels achieved a constant weight value.

2.5. In vitro MB release studies

Methylene blue (MB) was used as a model drug and was loaded during the stage of the preparation of the nanocomposites as described above. MB has been used as a model drug namely because it is a water-soluble dye that allows an immediate visual inspection of the test.

The release experiments were performed in a thermostatic orbital shaker KS 4000I Control from IKA at 37 °C and 120 rpm. A lyophilized disc was introduced in a glass beaker containing 50 mL PBS 0.01 M pH 7.4 and 0.05% (w/v) sodium azide as preserving agent. After predetermined intervals, 1.0 mL of the release medium was drawn and analyzed by UV–Vis spectroscopy (λ = 663 nm) to

determine the amount of MB released at each time point and replaced by 1 mL of fresh PBS to maintain the original volume. Prior to UV–Vis analysis the aliquot was diluted into KCl 1 M (dilution ratio 1:6) to ensure that the MB released did not interact with κ-carrageenan (Soedjak, 1994). The cumulative released fraction at time t (m_t/m_0) was calculated using Eq. (2)

$$\frac{m_t}{m_0} = \frac{50 \times C_n + \sum_{i=0}^{n-1} C_i}{m_0} \quad (2)$$

where m_t is the cumulative mass of MB released at time t, m_0 is the original mass of MB loaded, C_i is the mass concentration of MB (per mL) of the aliquot, C_n is the mass concentration of MB (per mL) of the aliquot at time t and n is the total number of aliquots extracted until time t. The release experiments were performed in triplicate.

The MB release of hydrogel nanocomposites was also carried out in PBS containing KCl 1 M following the same procedure. These experiments aimed to prevent the dissolution of κ-carrageenan during MB release and thus to better understand the role of the polymer matrix in the mechanism of release.

2.6. Instrumentation

2.6.1. X-ray diffraction (XRD)

X-ray power diffraction of Fe_3O_4 powders was performed using a Rigaku Geigerflex Dmax-C X-ray diffractometer (Japan) equipped with a Cu Kα monochromatic radiation source.

2.6.2. FTIR spectroscopy

FTIR spectra of carrageenan and carrageenan nanocomposites were collected using a spectrometer Mattson 7000 (USA) coupled to an horizontal attenuated total reflectance (ATR) cell, accumulating 256 scans and using a resolution of 4 cm^{-1}.

2.6.3. UV–Vis spectrophotometry

A Jasco V 560 UV/Vis spectrophotometer (Jasco Inc., USA) was used for recording the UV/Vis absorption spectra of the aliquots.

2.6.4. Scanning electron microscopy (SEM)

SEM analysis of blank hydrogel and carrageenan nanocomposites was performed using a scanning electron microscope Hitachi SU-70 at an accelerating voltage of 15 kV, using carbon sputtered samples.

2.6.5. Zeta potential measurements

The surface charge of magnetic nanoparticles was assessed by zeta potential measurements, using a Zetasizer Nanoseries instrument from Malvern Instruments (UK).

2.6.6. Dynamic mechanical analysis (DMA)

The DMA measurements of blank hydrogel and carrageenan nanocomposites were performed on a Tritec 2000 DMA dynamic mechanical analyser (Triton Technology Ltd., UK). The hydrogels were clamped between a parallel-plate compression clamp and an oscillatory deformation with amplitude of 10 μm and a frequency of 1 Hz was applied at various static forces ranging from 0.1 to 0.5 N. The elastic modulus was calculated from extrapolation of experimental data towards zero compression conditions as described elsewhere (Meyvis et al., 2002). DMA measurements were performed in triplicate.

2.7. Mathematical modeling of release kinetics

The *in vitro* drug release data were fitted to the Ritger–Peppas model (Ritger & Peppas, 1987), a semi-empirical power law described by Eq. (3)

$$\frac{m_t}{m_\infty} = k\,t^n \quad (3)$$

where m_t is the cumulative amount of drug released at time t, m_∞ is the cumulative amount of drug released at infinite time, k is a constant incorporating structural and geometric characteristics of the carrier and n is the release exponent indicative of the mechanism of drug release that depends also of the geometry of the carrier.

The above equation is a simple semi-empirical model that has two distinct physical realistic meanings for $n = 0.5$ and $n = 1.0$. When the release is driven by pure drug diffusion (Fick's law) n takes the value of 0.5. When $n = 1.0$ the drug release rate is constant in time and corresponds to zero-order release kinetics, also termed as case-II transport and the drug release follows a polymer chain relaxation mechanism (also designated as swelling controlled mechanism) (Fu & Kao, 2010; Siepmann & Peppas, 2001). Values of n between 0.5 and 1.0 indicate non-Fickian transport mechanism, generally termed as anomalous transport and can be understood as an indicator for the superposition of both phenomena (Fu & Kao, 2010; Siepmann & Peppas, 2001). For a radial diffusion from a cylindrical carrier such as used herein different values of n have been derived, being $n = 0.45$ and $n = 0.89$ for diffusion-controlled mechanism and case-II transport, respectively. Occasionally, values of $n > 0.89$ for release from cylinders have been observed, indicating super case-II transport. In this case the drug release follows a mechanism controlled by polymer relaxation and erosion, involving a relaxing boundary (dry glassy/hydrated rubbery polymer interface) moving into the matrix at an increasing rate (Cooke & Chen, 1995).

The cumulative fractional MB release data were fitted to Eq. (3) using the method of least squares.

2.8. Statistical analysis

Quantitative data are expressed as mean ± standard deviation from at least three independent experiments. Statistical comparisons were carried out using the one-way ANOVA test and multiple comparisons by the Tukey all pairwise approach with $P < 0.05$. These tests were performed using Minitab software (version 15).

3. Results and discussion

3.1. Characterization of κ-carrageenan nanocomposites

Magnetic iron oxide nanoparticles used as dispersed phase in carrageenan nanocomposites were synthesized by chemical co-precipitation of Fe(II) and Fe(III) ions. The XRD diffractogram (Fig. S1, Supplementary data) of the nanoparticles is consistent with the presence of magnetite (Fe_3O_4) as the main crystalline phase. The average nanoparticle diameter was estimated to be 17.4 ± 3.8 nm, using a modified version of Scherrer's equation (Borchert et al., 2005; Daniel-da-Silva et al., 2007).

Nanocomposites were prepared by homogeneous dispersion of Fe_3O_4 nanoparticles within a κ-carrageenan aqueous solution, followed by gelation of the mixture and by freeze-drying. The ATR-FTIR spectra of the nanocomposites (Fig. S2, Supplementary data) show the typical carrageenan absorption bands, namely around 1225 cm^{-1}, corresponding to the S–O asymmetric stretching mode, the two broad absorption bands, due to C–O and C–OH vibrations, observed in the 1040–1070 cm^{-1} region and a well-defined band at 845–850 cm^{-1} corresponding to the α(1–3)-D-galactose C–O–S stretch of the polysaccharide (Prado-Fernández, Rodríguez-

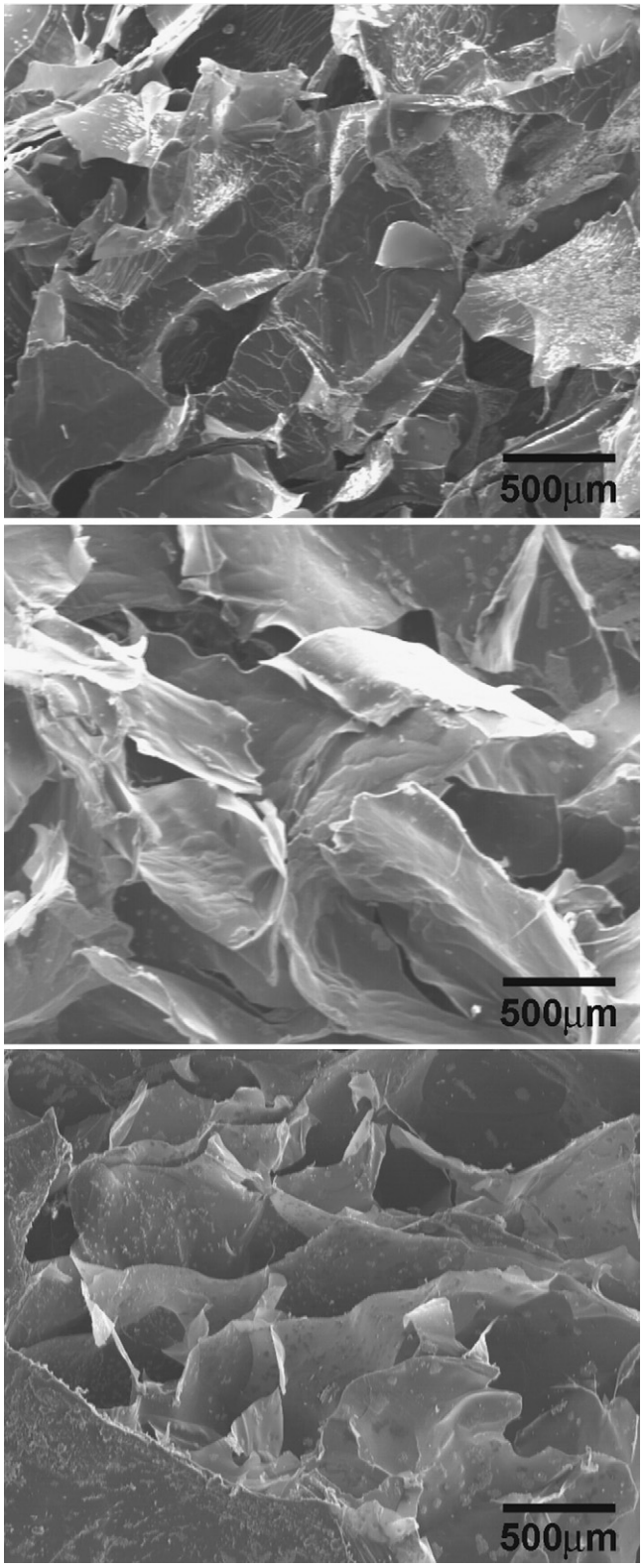

Fig. 2. SEM micrographs of lyophilized blank hydrogel K40 (top) and nanocomposites K40_MGN (centre) and K40_MGN100 (bottom).

Vázquez, Tojo, & Andrade, 2003). The incorporation of Fe_3O_4 nanoparticles and MB did not originate the shift of the carrageenan bands or the appearance of new band which in principle indicates the absence of significant interactions between the carrageenan and the MB and Fe_3O_4 nanoparticles. Note that for the MB and

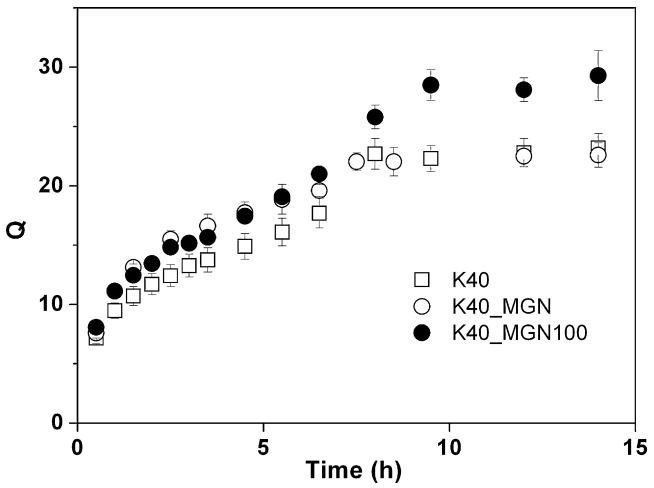

Fig. 3. Swelling ratio (Q) of the blank hydrogel and hydrogel nanocomposites in PBS as a function of time.

Fe_3O_4 concentrations used in this work, the corresponding vibrational bands are masked by the κ-carrageenan absorption bands used as matrix.

SEM observations of the lyophilized hydrogels were carried out in order to verify the effect of the NPs on the microstructure. Both blank hydrogel and nanocomposites show a continuous structure of irregular pores and high interconnectivity (Fig. 2). The pore size in the blank hydrogel (K40) ranges from several microns up to about 150 μm and was not significantly affected upon the addition of the Fe_3O_4 NPs.

3.2. Swelling of κ-carrageenan nanocomposites

Fig. 3 displays the swelling ratio (Q) in PBS as function of time for κ-carrageenan hydrogels with and without Fe_3O_4 nanoparticles. Hydrogel nanocomposites swell slightly faster than the blank hydrogel. However, the most striking differences are observed at the equilibrium. The equilibrium swelling ratio (Q_{equil}) of hydrogels remains invariable upon the incorporation of less Fe_3O_4 NPs load (up to 0.025%) while further addition of Fe_3O_4 NPs (K40_MGN100) results in an increase of the Q_{equil} from 22 to 29 (Fig. 3). Our previous studies on viscoelastic properties of κ-carrageenan/Fe_3O_4 nanocomposites have shown that the incorporation of increased Fe_3O_4 NPs content originates stronger κ-carrageenan hydrogels, as viewed from increased values of elastic modulus (Daniel-da-Silva et al., 2008). This was further confirmed in this work by DMA measurements of the hydrogels. The elastic modulus (E') was calculated from compression mode experiments. The incorporation of low amount of Fe_3O_4 NPs barely affected the elastic modulus of the hydrogels (Table 2). However, for increased Fe_3O_4 NPs content an increase of E' is observed indicating that the reinforcement of the structure of the carrageenan matrix increases with the amount of the Fe_3O_4 NPs within the gel.

These results show that stronger hydrogels do not swell less, as it could be initially expected based on the equilibrium swelling theory (Peppas et al., 2000). The swelling of polyelectrolyte hydrogels

Table 2
The elastic modulus (E') of blank hydrogel and nanocomposites determined from compression DMA measurements.

Hydrogel	E' [kPa]
K40	147.0 ± 11.2
K40_MGN	143.0 ± 13.9
K40_MGN100	181.4 ± 8.5

such as κ-carrageenan is not only affected by the elastic properties of the polymeric network, but also by the ionic character of the hydrogel and of the surrounding media (Goponenko & Asher, 2005; Peppas et al., 2000; Rička & Tanaka, 1984). Since the carrageenan concentration and the release media composition was kept constant, a possible explanation may be related to the surface charge of Fe_3O_4 NPs used as nanofillers. At the pH of the carrageenan solution (pH 8.5–9.0) the zeta potential of the Fe_3O_4 nanoparticles was -21.8 ± 0.5 mV. The results indicate that the immobilization of surface charged Fe_3O_4 NPs within κ-carrageenan results in an afflux of water which causes the hydrogel to swell and are in agreement with previous observations in hydrogels containing gold and silver NPs (Saravanan, Padmanabha Raju, & Alam, 2007; Wang, Flynn, & Langer, 2004). The phenomenon was identified as Donnan effect of polyelectrolyte gels, and consists in the afflux of water to balance the osmotic pressure build-up caused by the immobilization of the surface charge NPs. The degree of osmotic swelling depends on the amount of charges immobilized within the gel and is proportional to the surface charge and concentration of the nanofillers. Thus, hydrogel nanocomposites with high load of Fe_3O_4 NPs swell more as viewed in Fig. 3, despite having a stronger structure.

When the surrounding medium was replaced by a buffered solution rich in K^+ ions, Q_{equil} was found to be 4.1 ± 0.5 for the blank hydrogel and 7.5 ± 2.1 and 5.2 ± 1.1 for K40_MGN and K40_MGN100 hydrogel nanocomposites, respectively. These results are significantly lower than Q_{equil} values observed in PBS and indicate that high K^+ concentration of the surrounding medium limits the swelling of carrageenan hydrogels.

3.3. *In vitro* MB release profiles

The amount of MB released was monitored by measuring the absorbance of the release medium at 663 nm, i.e. at the wavelength of maximum absorbance for MB. However, in aqueous medium MB interacts with κ-carrageenan and forms a water-soluble complex with absorption maximum at 559 nm (Soedjak, 1994) which may interfere with the quantitative determination of MB released. The complexation of MB and κ-carrageenan is reversible at high ionic strength values (Soedjak, 1994). This was further confirmed in our work upon the addition of KCl to the aliquots prior to UV/Vis analysis. The addition of KCl results in the disappearance of the absorbance of the complex at 559 nm and in the increase of the absorbance of the free MB at 617 and 663 nm (Fig. S3, supplementary data) and guarantees that the MB released is not interacting with κ-carrageenan and can be quantified by measuring the absorbance at 663 nm. The effects of the matrix composition (biopolymer and K^+ ions concentration) and of the load of Fe_3O_4 nanoparticles on the MB release profiles were evaluated.

3.3.1. *Effect of matrix composition*

Fig. 4 shows the release profiles of MB in PBS from κ-carrageenan hydrogels prepared with varied concentrations of biopolymer and K^+ ions. All the compositions evaluated exhibited a sustainable MB release. The release is faster in the first 2 h (burst release) and then progresses at lower rate until a steady concentration is achieved. Both κ-carrageenan and K^+ concentration were seen to affect the release profile. MB release rate is lower for increasing concentrations of both κ-carrageenan and K^+ ions, the latter having a more marked effect. The strength of κ-carrageenan gels is well known to increase for higher concentrations of biopolymer and of counterion (Piculell, 1995), thus the results observed follow the trend of the strength of the gel, stronger gels resulting in slower MB release. A similar relation between the gel strength and the release kinetics

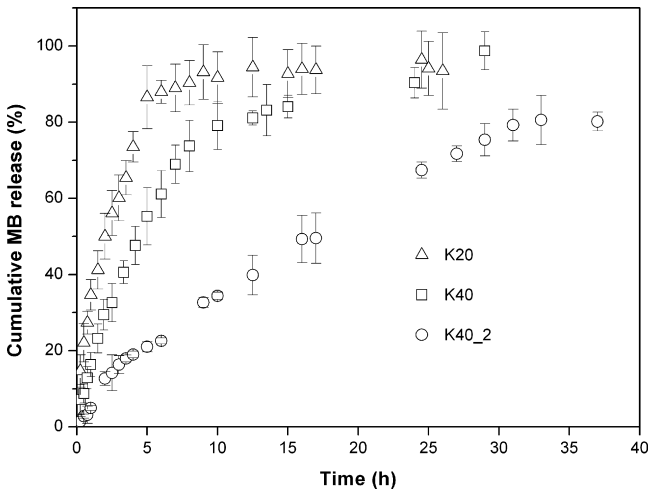

Fig. 4. *In vitro* MB release profiles in PBS from blank hydrogels prepared with varying concentrations of κ-carrageenan and K^+ ions.

in κ-carrageenan gels prepared by varying the counterion nature has been reported (Mangione et al., 2007).

3.3.2. *Effect of Fe_3O_4 NPs load*

Fig. 5a displays the *in vitro* release patterns of MB in PBS from κ-carrageenan/Fe_3O_4 composite discs. The release profile of the

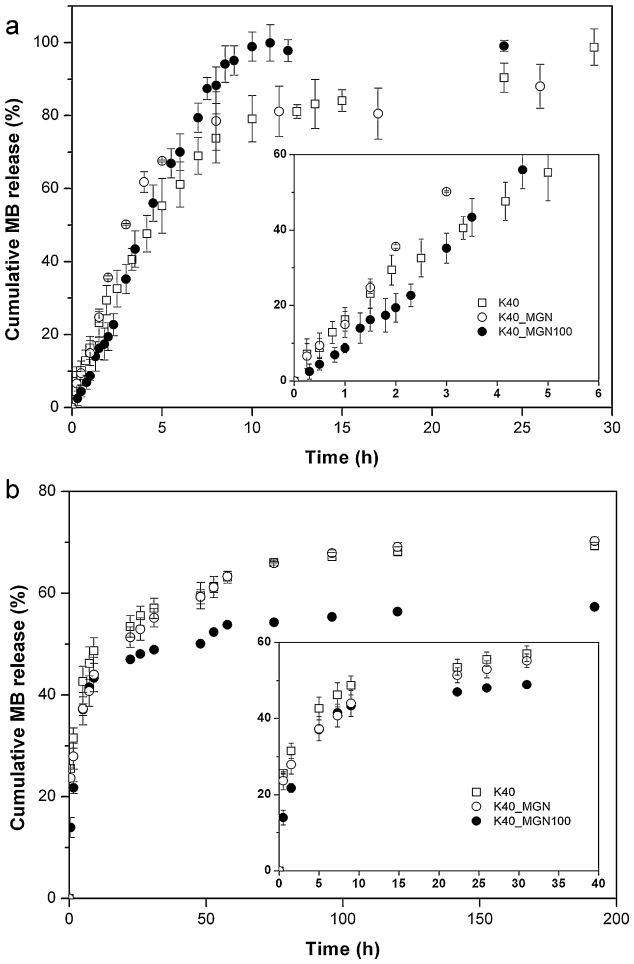

Fig. 5. *In vitro* MB release profiles from the blank hydrogel (K40) and hydrogel nanocomposites containing variable loads of Fe_3O_4 NPs in (a) PBS and in (b) PBS with K^+ 1 M. Inset: detail of the release profiles for the first 6 h (a) and 40 h (b).

Table 3
Parameters k and n, as estimated from the application of the Ritger–Peppas model to the data of MB release in PBS, and coefficient of determination (R^2).

Sample	$k \times 10^3$ [min^{-n}]	n	R^2
K20	33.3 ± 2.65	0.56 ± 0.02	0.998
K40	8.32 ± 0.92	0.74 ± 0.02	0.997
K40_2	3.40 ± 0.42	0.72 ± 0.02	0.995
K40_MGN	4.20 ± 1.09	0.91 ± 0.05	0.994
K40_MGN100	0.66 ± 0.13	1.20 ± 0.04	0.995

composite with less Fe_3O_4 NPs load (K40_MGN) is very similar to the profile observed for κ-carrageenan (K40), thus indicating that NPs loads of 0.025 wt% do not affect significantly the release profile of MB. Further addition of Fe_3O_4 NPs results in several differences. For K40_MGN100 the release at initial stage is slower than in the blank hydrogel and then progresses to a more rapid release at later stage before leveling, thus resulting in a sigmoidal profile (Fig. 5a). The maximum of MB released in K40_MGN100 is higher and happens earlier than in the blank hydrogel. This is in agreement with the swelling results that showed a significant increase of the equilibrium swelling ratio for this nanocomposite. The transport of the MB from the matrix to the surrounding medium is facilitated in the swollen matrix.

During *in vitro* release tests in PBS, the swelling of the hydrogel was clearly observed, leading to release of MB to the surrounding fluid, as simply noted by the bluish color acquired by the bulk solution. The hydrogel swelling was observed as the gradual dissolution of the polymer occurred, until complete dissolution occurred for prolonged times of the experiment. This behavior was expected as the κ-carrageenan hydrogels prepared here are non-covalent gels, whose polysaccharide chains are held together via electrostatic interactions between sulfate groups of carrageenan and K^+ ions.

In order to prevent the dissolution of the hydrogel discs, the release experiments from hydrogel nanocomposites were also performed in PBS having high K^+ ions concentration (1 M). The release profiles are shown in Fig. 5b and show, first, that the MB release was prolonged in time. Second, it is observed that the maximum of MB released in K40_MGN100 is lower than in the blank hydrogel, in opposition to the behavior observed in PBS. Since K40_MGN100 gels have higher elastic moduli than blank hydrogel (Table 2), these results indicate that at high K^+ concentration, the MB release rate follows the trend of the gel strength, i.e. stronger gels limit MB release. Besides preventing the dissolution of the polymer, the high concentration of K^+ ions in the surrounding medium restricts the swelling of the hydrogels. Thus, under these conditions the effect of the strength of the gel network in MB release prevails.

3.4. Kinetic studies

From the analysis of MB release profiles it is evident that different phenomena may control the drug release. The release of MB may be controlled either by MB diffusion or by the swelling and dissolution of the polymer, or combinations of these phenomena. In other words, the rate-limiting step for controlled release of the incorporated drug might be the diffusion of the model drug or the swelling and dissolution of the polymer matrix.

With the aim of gaining insight into the release mechanism, the experimental release data were fitted to the Ritger–Peppas model (Eq. (3)) for $(m_t/m_\infty) \leq 0.6$. The constant k and the exponent n estimated for each system as well as the corresponding coefficient of determination (R^2) are listed in Table 3. Overall the data fit well this model as R^2 was greater than 0.99 for all the systems.

The n value found for the release of MB from K20 hydrogels is greater than 0.45 and much smaller than 0.89, which suggests anomalous release, i.e. the polymer relaxation time is comparable to the diffusion time and the release behavior follows both diffusion and polymer relaxation controlled kinetics (Fu & Kao, 2010). When carrageenan concentration is double (sample K40) the value of n increases from 0.56 to 0.74, hence indicating that the release tends to be controlled by polymer relaxation. This is well in line with the fact that the strength of carrageenan gels increases with biopolymer concentration (Piculell, 1995). Increasing polymer fraction results in the formation of a denser network structure which will hinder the transport of the encapsulated drug to the surrounding liquid, as previously found for other hydrogels (Amsden, 1998). No significant variation of n was noted when K^+ concentration increased from 1 to 2 M which suggests that the K^+ ions content does not affect the mechanism of release within the range of K^+ concentrations studied. However, it should be pointed out that the values of K^+ concentration refer to the solution used for preparing hydrogels. The actual K^+ content on hydrogels should be lower since some of the aqueous phase, comprising water and most probably dissolved ions, has been expelled by the network of the gel over time, in a phenomenon called syneresis (Ramakrishnan, Gerardin, & Prud'homme, 2004). The comparison of k values indicates that the release rate is slower for the hydrogel with the highest K^+ content, which is in agreement with the drug release observations.

The incorporation of Fe_3O_4 NPs (0.025 wt%) originates an increase of the exponent n to 0.91, very close to 0.89 which indicates case II transport, i.e. the release becomes controlled by polymer chain relaxation. These results suggest that the incorporation of Fe_3O_4 NPs restricts the relaxation of carrageenan molecules. This observation is in agreement with DMA results and our previous findings for the rheological properties of magnetic carrageenan nanocomposites (Daniel-da-Silva et al., 2008). The combined effect of negatively surface charged magnetite nanoparticles and K^+ ions promotes a more extensive carrageenan helical aggregation and leads to stronger gels (Daniel-da-Silva et al., 2008). The restriction of the polymer relaxation is believed to affect the MB transport to the surrounding medium, thus leading to a mechanism controlled by polymer relaxation. This is similar to an effect noted for hydroxyapatite/chitosan nanocomposites (Liu, Chen, Li, & Liu, 2006) in which the incorporation of Ca-deficient hydroxyapatite nanoparticles was seen to reduce the relaxation of chitosan molecules and to shift the drug release from a diffusion-controlled towards polymer relaxation-controlled mechanisms.

Further increase in Fe_3O_4 content originates n values significantly larger than 1, which are well in line with the sigmoidal release profile observed for these nanocomposites and indicate super case II transport. The underlying mechanism is a polymer relaxation and erosion controlled mechanism that has been identified in systems with increased solvent availability in the matrix (Charoenthai, Kleinebudde, & Puttipipatkhachorn, 2007; Soo et al., 2008). This has been ascribed to an increased water plasticization at the relaxing boundary (Sriamornsak, Thirawong, & Korkerd, 2007), hence in agreement with the high values of equilibrium swelling observed here for K40_MGN100 (Fig. 3). The sigmoidal release profile of these nanocomposites comprises (i) an initial stage wherein the release rate is lower than in the blank hydrogel followed by (ii) the release acceleration at a later stage, before reaching a plateau (Fig. 5). The retard in the initial drug release is most likely due to the formation of stronger gels upon the addition of Fe_3O_4 NPs (Daniel-da-Silva et al., 2008) as dispersed phase. A similar retarding release effect with increasing hydrogel crosslinking has been reported in Ca^{2+} crosslinked pectin pellets (Wei, Sun, Wu, Yin, & Wu, 2006).

The acceleration of the release observed at a later stage is most probably due to an increased plasticized effect due to the water permeation into the matrix as previously observed in other systems following a super case II release kinetics (Charoenthai, Kleinebudde, & Puttipipatkhachorn, 2007; Soo et al., 2008; Sriamornsak, Thirawong, & Korkerd, 2007). The swelling

results have revealed high swelling ratio due to the incorporation of surface charged Fe_3O_4 NPs (Fig. 3). The additional water uptake should result in the formation of additional pores and in the enlargement of the current existing pores, giving rise to more free volume for the transport of the encapsulated drug and to the acceleration of the release, as proposed by Soo et al. (2008) in drug release from chitosan based implants. Moreover, matrix erosion can arise from the high degree of swelling, resulting in a very rapid drug release at this stage (Asghar, Azeemuddin, Jain, & Chandran, 2009; Wei et al., 2006).

4. Conclusions

The effect of the Fe_3O_4 NPs as nanofillers in the swelling of κ-carrageenan hydrogels and methylene blue (MB) release mechanism and kinetics from κ-carrageenan nanocomposites have been investigated. The incorporation of Fe_3O_4 NPs was seen to increase the swelling of κ-carrageenan hydrogels, in spite of the high viscoelastic moduli of the resulting nanocomposites. It is proposed that for high NPs load tested, the effect of the afflux of water to balance the osmotic pressure build-up caused by the immobilization of the surface charged NPs prevails the effect of the reinforcement of the gel network. While the release of MB from κ-carrageenan hydrogel followed an anomalous transport, it tended to be controlled by polymer relaxation if Fe_3O_4 NPs are incorporated as dispersed phase. The release kinetics depended on the Fe_3O_4 NPs load and was found to be case II and super case II transport for low and high Fe_3O_4 NPs content, respectively. Considering that increasing Fe_3O_4 NPs content results in stronger gels and higher swelling ratios, these having opposite effects on release rate, it is suggested that the mechanism of MB release from κ-carrageenan nanocomposites is primarily determined by the balance between the effect of the dispersed phase on the strength of the hydrogel network and the extent of swelling. These results indicate that the incorporation of nanoparticles within polyelectrolyte hydrogels is a valuable route for tailoring the release rate of encapsulated drugs and have broad implications in the design of novel biomaterials for controlled drug release.

Acknowledgements

We thank the RNME (National Electronic Microscopy Network) for SEM images. The authors acknowledge FCT, FSE and POPH for funding.

Appendix A. Supplementary data

Supplementary data associated with this article can be found, in the online version, at doi:10.1016/j.carbpol.2011.07.051.

References

Amsden, B. (1998). Solute diffusion within hydrogels. Mechanisms and models. *Macromolecules*, *31*, 8382–8395.

Asghar, L. F. A., Azeemuddin, Md., Jain, V., & Chandran, S. (2009). Design and in vitro evaluation of formulations with pH and transit time controlled sigmoidal release profile for colon-specific delivery. *Drug Delivery*, *16*, 295–303.

Bertoglio, P., Jacobo, S. E., & Daraio, M. E. (2010). Preparation and characterization of PVA films with magnetic nanoparticles: The effect of particle loading on drug release behavior. *Journal of Applied Polymer Science*, *115*, 1859–1865.

Borchert, H., Shevchenko, E. V., Robert, A., Mekis, I., Kornowski, A., Grübel, G., et al. (2005). Determination of nanocrystal sizes: A comparison of TEM, SAXS, and XRD studies of highly monodisperse $CoPt_3$ particles. *Langmuir*, *21*, 1931–1936.

Charoenthai, N., Kleinebudde, P., & Puttipipatkhachorn, S. (2007). Use of chitosan–alginate as alternative pelletization aid to microcrystalline cellulose in extrusion/spheronization. *Journal of Pharmaceutical Sciences*, *96*, 2469–2484.

Cooke, N. E., & Chen, C. (1995). A contribution to a mathematical theory for polymer-based controlled release devices. *International Journal of Pharmaceutics*, *115*, 17–27.

Daniel-da-Silva, A. L., Ferreira, L., Gil, A. M., & Trindade, T. (2011). Synthesis and swelling behavior of temperature responsive k-carrageenan nanogels. *Journal of Colloid and Interface Science*, *355*, 512–517.

Daniel-da-Silva, A. L., Fateixa, S., Guiomar, A. J., Costa, B. F. O., Silva, N. J. O., Trindade, T., et al. (2009). Biofunctionalized magnetic hydrogel nanospheres of magnetite and k-carrageenan. *Nanotechnology*, *20*, 355602.

Daniel-da-Silva, A. L., Lóio, R., Lopes-da-Silva, J. A., Trindade, T., Goodfellow, B. J., & Gil, A. M. (2008). Effects of magnetite nanoparticles on the thermorheological properties of carrageenan hydrogels. *Journal of Colloid and Interface Science*, *324*, 205–211.

Daniel-da-Silva, A. L., Trindade, T., Goodfellow, B. J., Costa, B. F. O., Correia, R. N., & Gil, A. M. (2007). In situ synthesis of magnetite nanoparticles in carrageenan gels. *Biomacromolecules*, *8*, 2350–2357.

Frimpong, R. A., & Hilt, J. Z. (2007). Hydrogel nanocomposites for intelligent therapeutics. In N. A. Peppas, J. Z. Hilt, & J. B. Thomas (Eds.), *Nanotechnology in therapeutics: Current technology and applications* (pp. 241–256). United Kingdom: Horizon Bioscience.

Fu, Y., & Kao, W. J. (2010). Drug release kinetics and transport mechanisms of non-degradable and degradable polymeric delivery systems. *Expert Opinion on Drug Delivery*, *7*, 429–444.

Goponenko, A. V., & Asher, S. (2005). Modeling of stimulated hydrogel volume changes in photonic crystal Pb^{2+} sensing materials. *Journal of the American Chemical Society*, *127*, 10753–10759.

Gupta, V. K., Hariharan, M., Wheatley, T. A., & Price, J. C. (2001). Controlled-release tablets from carrageenans: Effect of formulation, storage and dissolution factors. *European Journal of Pharmaceutics and Biopharmaceutics*, *51*, 241–248.

Hamidi, M., Azadi, A., & Rafiei, P. (2008). Hydrogel nanoparticles in drug delivery. *Advanced Drug Delivery Review*, *60*, 1638–1649.

Hoare, T. R., & Kohane, D. S. (2008). Hydrogels in drug delivery: Progress and challenges. *Polymer*, *49*, 1993–2007.

Hu, S.-H., Liu, T.-Y., Liu, D.-M., & Chen, S.-Y. (2007). Nano-ferrosponges for controlled drug release. *Journal of Controlled Release*, *121*, 181–189.

Keppeler, S., Ellis, A., & Jacquier, J. C. (2009). Cross-linked carrageenan beads for controlled release delivery systems. *Carbohydrate Polymers*, *78*, 973–977.

Leong, K. H., Chung, L. Y., Noordin, M. I., Mohamad, K., Nishikawa, M., Onuki, Y., et al. (2011). Carboxymethylation of kappa-carrageenan for intestinal-targeted delivey of bioactive macromolecules. *Carbohydrate Polymers*, *83*, 1507–1515.

Lin, C.-C., & Metters, A. T. (2006). Hydrogels in controlled release formulations: Network design and mathematical modeling. *Advanced Drug Delivery Review*, *58*, 1379–1408.

Liu, Y., Zhu, Y.-Y., Wei, G., & Lu, W.-Y. (2009). Effect of carrageenan on poloxamer-based in situ gel for vaginal use: Improved in vitro and in vivo sustained-release properties. *European Journal of Pharmaceutical Sciences*, *37*, 306–312.

Liu, T.-Y., Chen, S.-Y., Li, J.-H., & Liu, D.-M. (2006). Study on drug release behaviour of CDHA/chitosan nanocomposites-effect of CDHA nanoparticles. *Journal of Controlled Release*, *112*, 88–95.

Liu, T.-Y., Hu, S.-H., Liu, T.-Y., Liu, D.-M., & Chen, S.-Y. (2006). Magnetic-sensitive behaviour of intelligent ferrogels for controlled release of drug. *Langmuir*, *22*, 5974–5978.

Mangione, M. R., Giacomazza, D., Cavallaro, G., Bulone, D., Martorana, V., & San Biagio, P. L. (2007). Relation between structural and release properties in a polysaccharide gel system. *Biophysical Chemistry*, *129*, 18–22.

Meyvis, T. K. L., Stubbe, B. G., Van Steenbergen, M. J., Hennink, W. E., De Smedt, S. C., & Demeester, J. (2002). A comparison between the use of dynamic mechanical analysis and oscillatory shear rheometry for the characterisation of hydrogels. *International Journal of Pharmaceutics*, *244*, 163–168.

Mohamadnia, Z., Zohuriaan-Mehr, M. J., Kabiri, K., Jamshidi, A., & Mobedi, H. (2007). pH-sensitive IPN hydrogel beads of carrageenan-alginate for controlled drug delivery. *Journal of Bioactive and Compatible Polymers*, *22*, 342–356.

Nannaki, S., Karava, E., Kalantzi, L., & Bikiaris, D. (2010). Miscibility study of carrageenan blends and evaluation of their effectiveness as sustained release carriers. *Carbohydrate Polymers*, *79*, 1157–1167.

Peppas, N. A., Bures, P., Leobandung, W., & Ichikawa, H. (2000). Hydrogels in pharmaceutical formulations. *European Journal of Pharmaceutics and Biopharmaceutics*, *50*, 27–46.

Piculell, L. (1995). Gelling carrageenans. In A. M. Stephen (Ed.), *Food polysaccharides and their applications* (pp. 205–217). New York: Marcel Dekker.

Polyak, B., & Friedman, G. (2009). Magnetic targeting for site-specific drug delivery: Applications and clinical potential. *Expert Opinion on Drug Delivery*, *6*, 53–70.

Prado-Fernández, J., Rodríguez-Vázquez, J. A., Tojo, E., & Andrade, J. M. (2003). Quantitation of κ-, ι- and λ-carrageenans by mid-infrared spectroscopy and PLS regression. *Analytica Chimica Acta*, *480*, 23–37.

Ramakrishnan, S., Gerardin, C., & Prud'homme, R. K. (2004). Syneresis of carrageenan gels: NMR and rheology. *Soft Materials*, *2*, 145–153.

Rasool, N., Yasin, T., Heng, J. Y. Y., & Akhter, Z. (2010). Synthesis and characterization of novel pH-, ionic strength and temperature-sensitive hydrogel for insulin delivery. *Polymer*, *51*, 1687–1693.

Rička, J., & Tanaka, T. (1984). Swelling of ionic gels: Quantitative performance of the Donnan theory. *Macromolecules*, *17*, 2916–2921.

Ritger, P. L., & Peppas, N. A. (1987). A simple equation for description of solute release. I. Fickian and non-Fickian release from non-swellable devices in the form of slabs, spheres, cylinders or discs. *Journal of Controlled Release*, *5*, 23–36.

Saboktakin, M. R., Tabatabaie, R., Maharramov, A., & Ramazanov, M. A. (2010). Synthesis and characterization of superparamagnetic chitosan-dextran sulfate hydrogels as nanocarriers for colon-specific drug delivery. *Carbohydrate Polymers*, *81*, 372–376.

Sankalia, M. G., Mashru, R. C., Sankalia, J. M., & Sutariya, V. B. (2006). Stability improvement of alpha-amylase entrapped in kappa-carrageenan beads: Physicochemical characterization and optimization using composite index. *International Journal of Pharmaceutics*, *312*, 1–14.

Santo, V. E., Frias, A. M., Carida, M., Cancedda, R., Gomes, M. E., Mano, J. F., et al. (2009). Carrageenan-based hydrogels for the controlled delivery of PDGF-BB in bone tissue engineering applications. *Biomacromolecules*, *10*, 1392–1401.

Saravanan, P., Padmanabha Raju, M., & Alam, S. (2007). A study on synthesis and properties of Ag nanoparticles immobilized polyacrylamide hydrogel composites. *Materials Chemistry and Physics*, *103*, 278–282.

Satarkar, N. S., Biswal, D., & Hilt, J. Z. (2010). Hydrogel nanocomposites: A review of applications as remote controlled biomaterials. *Soft Matter*, *6*, 2364–2371.

Siepmann, J., & Peppas, N. A. (2001). Modeling of drug release from delivery systems based on hydroxypropyl methylcellulose (HPMC). *Advanced Drug Delivery Review*, *48*, 139–157.

Shen, F., Poncet-Legrand, C., Somers, S., Slade, A., Yip, C., Duft, A. M., et al. (2005). Properties of a novel magnetized alginate for magnetic resonance imaging. *Biotechnology and Bioengineering*, *83*, 282–292.

Soedjak, H. S. (1994). Colorimetric determination of carrageenans and other anionic hydrocolloids with methylene blue. *Analytical Chemistry*, *66*, 4514–4518.

Soo, P. L., Cho, J., Grant, J., Ho, E., Piquette-Miller, M., & Allen, C. (2008). Drug release mechanism of paclitaxel from a chitosan-lipid implant system: Effect of swelling, degradation and morphology. *European Journal of Pharmaceutics and Biopharmaceutics*, *69*, 149–157.

Sriamornsak, P., Thirawong, N., & Korkerd, K. (2007). Swelling, erosion and release behaviour of alginate-based matrix tablets. *European Journal of Pharmaceutics and Biopharmaceutics*, *66*, 435–450.

Tapia, C., Corbalan, V., Costa, E., Gai, M. N., & Yazdani-Pedram, M. (2005). Study of the release mechanism of diltiazem hydrochloride from matrices based on chitosan-alginate and chitosan-carrageenan mixtures. *Biomacromolecules*, *6*, 2389–2395.

Wang, C., Flynn, N. T., & Langer, R. (2004). Controlled structure and properties of the thermoresponsive nanoparticle-hydrogel composites. *Advanced Materials*, *16*, 1074–1079.

Wei, X., Sun, N., Wu, B., Yin, C., & Wu, W. (2006). Sigmoidal release of indomethacin from pectin matrix tablets: Effect of in situ crosslinking by calcium cations. *International Journal of Pharmaceutics*, *318*, 132–138.

Zrínyi, M. (2000). Intelligent polymer gels controlled by magnetic fields. *Colloid and Polymer Science*, *278*, 98–103.